ACS APPLIED MATERIALS & INTERFACES

www.acsami.org

Research Article

Label-Free Analysis of Multivalent Protein Binding Using Bioresponsive Nanogels and Surface Plasmon Resonance (SPR)

Hae Min Yang, Jie Ying Teoh, Guk Hee Yim, Yongdoo Park, Young Gyu Kim, Jongseong Kim,* and Dongwon Yoo*

Cite This: *ACS Appl. Mater. Interfaces* 2020, 12, 5413−5419

Read Online

ACCESS | Metrics & More | Article Recommendations | Supporting Information

ABSTRACT: Precise identification of protein−protein interactions is required to improve our understanding of biochemical pathways for biology and medicine. In physiology, how proteins interact with other proteins or small molecules is crucial for maintaining biological functions. For instance, multivalent protein binding (MPB), in which a ligand concurrently interacts with two or more receptors, plays a key role in regulating complex but accurate biological functions, and its interference is related to many diseases. Therefore, determining MPB and its kinetics has long been sought, which currently requires complicated procedures and instruments to distinguish multivalent binding from monovalent binding. Here, we show a method for quickly evaluating the MPB over monovalent binding and its kinetic parameters in a label-free manner. Engaging pNIPAm-*co*-AAc nanogels with MPB-capable moieties (e.g., PD-1 antigen and biocytin) permits a surface plasmon resonance (SPR) instrument to evaluate the MPB events by amplifying signals from the specific target molecules. Using our MPB-based method, PD-1 antibody that forms a type of MPB by complexing with two PD-1 proteins, which are currently used for cancer immunotherapy, is detectable down to a level of 10 nM. In addition, small multivalent cations (e.g., Ca^{2+}, Fe^{2+}, and Fe^{3+}) are distinguishably measurable over monovalent cations (e.g., Na^{+} and K^{+}) with the pNIPAm-*co*-AAc nanogels.

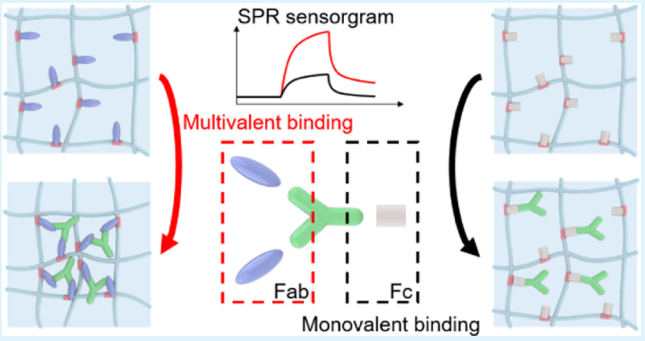

KEYWORDS: *hydrogel, protein−protein interaction, protein multivalent binding (PMB), label free, biosensor, surface plasmon resonance*

1. INTRODUCTION

A method to identify protein interactions with other proteins or molecules is central for better understanding of biochemical pathways in biology and medicine.[1] Developing novel biochemical and biophysical techniques has led to advances not only in elucidating the molecular basis of biological functions but also in discovering targeted drug molecules.[2] Kinetic analysis of protein binding in real time is fundamental to developing new drugs and medical treatments.[3−6] In parallel, detection of a target molecule without prelabeling steps has been highly advantageous for many practical applications due to not only its experimental ease but also the fact that the labeling can perturb binding events and results.[7−10]

In physiology, proteins are often assembled in various complexes by binding to other proteins, which is a prerequisite for complex but accurate biological functions.[11,12] In terms of formulation, protein binding is divided into two groups where either one protein molecule interacts with one molecule, i.e., monovalent protein binding,[13] or one molecule concurrently binds with more than two molecules, i.e., multivalent protein binding (MPB).[14,15] Immunoglobulin G (IgG), i.e., the most common antibody in human serum and medical treatment, is composed of two identical antigen binding sites, resulting in a protein ternary complex by divalent binding, a type of MPB.[16,17] Cell signaling by epidermal growth factor (EGF) is also triggered by receptor dimerization through MPB, which plays a key role in cancer development.[18] However, there is no efficient method to determine MPB and its kinetic values in a label-free manner. For instance, isothermal titration calorimetry (ITC) has been used to quantify thermodynamic parameters of protein interactions and thereby sense multivalent protein complexes.[19,20] One limitation of this methodology is its prerequisite for a large amount of purified proteins.

Surface plasmon resonance (SPR) has been regarded as a gold standard technique for estimating protein interactions with drug molecules such as humanized antibodies, small molecules, and purified proteins.[21−24] Although the use of SPR instruments allows us to determine the kinetic values of participating molecules, there are a number of caveats

Received: September 24, 2019
Accepted: January 3, 2020
Published: January 3, 2020

https://dx.doi.org/10.1021/acsami.9b17328
ACS Appl. Mater. Interfaces 2020, 12, 5413−5419

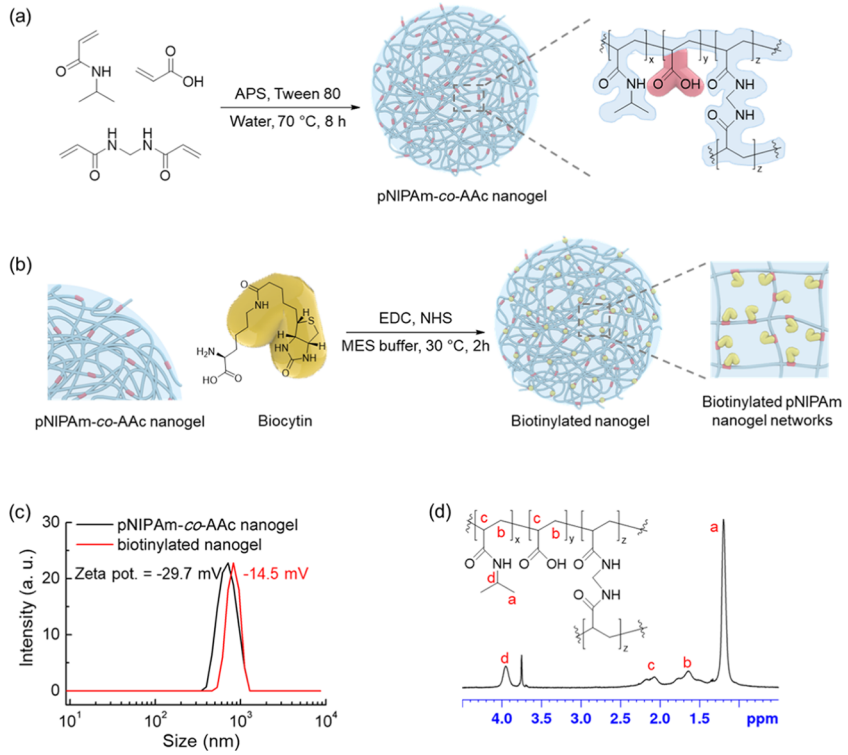

Figure 1. Schematics of nanogel synthesis and identification. (a) Synthetic routes for pNIPAm-*co*-AAc nanogels. (b) Their functionalization with biocytin via EDC coupling. (c) Size and surface charge of the nanogels (before and after functionalization) analyzed by dynamic light scattering (DLS) and ζ-potential measurement, respectively. (d) NMR spectra of pNIPAm-*co*-AAc nanogels.

concerning the fidelity of the measurement for complex samples, small compounds, and highly hydrophobic molecules. In addition, these instruments are unable to distinguish multivalent binding from monovalent binding. Therefore, it will be extremely valuable if we develop an easy and reliable method of using a SPR instrument that can measure the MPB in a quantitative and label-free manner.

To develop an efficient biochemical sensing platform for MPB identification and kinetics, we utilized bioresponsive hydrogel nanoparticles (nanogels). Hydrogels have been extensively investigated for optical elements,[25] drug delivery,[26,27] artificial cells,[28] and biosensors.[29,30] In particular, biologically functionalized hydrogel microparticles were demonstrated to have the capability of distinguishing MPB from nonspecific and monovalent binding events using the change in the image of surface-immobilized microparticles.[29,31] However, this image-based analysis attenuated the sensitivity for a target molecule in MPB detection and lacked precise quantitative information due to its dependence on visible changes in microgels. Here, we develop a method to clearly evaluate MPB events with kinetic parameters by engaging bioresponsive pNIPAm-*co*-AAc nanogels with a SPR instrument. Our results show that PD-1 antibody that participates in MPB with two PD-1 antigens is detectable down to a level of 10 nM. In addition, even small divalent and trivalent cations, which are unable to differentiate responding signals with conventional SPR analysis, are distinguishably measurable over monovalent cations using our MPB-based method.

2. MATERIALS AND METHODS

2.1. Materials. All chemical compounds were used as received without further purification unless otherwise stated. *N*-Isopropylacrylamide (NIPAm), acrylic acid (AAc), *N*,*N*′-methylenebisacrylamide (BIS), ammonium persulfate (APS), poly(oxyethylene) sorbitan monooleate (Tween 80), *N*-hydroxysuccinimide (NHS), biocytin, and bovine serum albumin (BSA) were purchased from Sigma-Aldrich (St. Louis, MO). 1-Ethyl-3-(3-dimethylaminopropyl)carbodiimide (EDC) was purchased from Thermo Fisher Scientific (Waltham, MA). PD-1 protein, PD-1 IgG antibodies, and protein A were purchased from Sino Biological Inc. (Wayne, PA). Cy2-streptavidin was purchased from Jackson ImmunoResearch (West Grove, PA). The water used throughout this study was distilled and deionized to 18.2 MΩ cm (aquaMAX-Ultra 370 water purification system, Young In, Anyang, Korea) and filtered with a 0.22 μm filter to remove particulate matter. 2-(*N*-Morpholino)ethanesulfonic acid (MES) and 0.9% sodium chloride buffer were purchased from Thermo Fisher Scientific. Phosphate-buffered saline (PBS, 1×) without calcium or magnesium was purchased from GE Healthcare (Chicago, IL).

2.2. Synthesis of the Hydrogel Nanoparticles (Nanogels). Nanogels were prepared via aqueous free-radical precipitation polymerization with slight modifications from previously reported literature procedures.[29] In short, the total monomer concentration was fixed at 100 mM, with a total reaction volume of 100 mL. The AAc and BIS contents were adjusted to 10 and 2%, respectively, relative to the total monomer concentration. The solution mixture was prepared by dissolving NIPAm and BIS in deionized water and then adding Tween 80, yielding a total surfactant concentration of 0.5 mM. The monomer solution was filtered with a 0.22 μm syringe-driven filter and subsequently transferred to a 100 mL three-neck round-bottomed flask equipped with a reflux condenser, a thermometer, and a magnetic stirring bar. Once equilibrated to 70 °C, the reaction mixture was purged with Ar while stirring at 275 rpm. After 1 h, the solution of AAc was added to the mixture by pipetting, and Ar purging was maintained for 10 min before the initiation of polymerization. Polymerization was initiated by syringe injection of a 0.2 mL aliquot of 1 mM APS into the reaction vessel. The reaction was allowed to proceed for 6 h at 70 °C under continuous Ar purging with stirring. After cooling, the resulting product was purified by dynamic dialysis (Spectra/Por Tube-A-Lyzer, MWCO 100 kD,

https://dx.doi.org/10.1021/acsami.9b17328
ACS Appl. Mater. Interfaces 2020, 12, 5413−5419

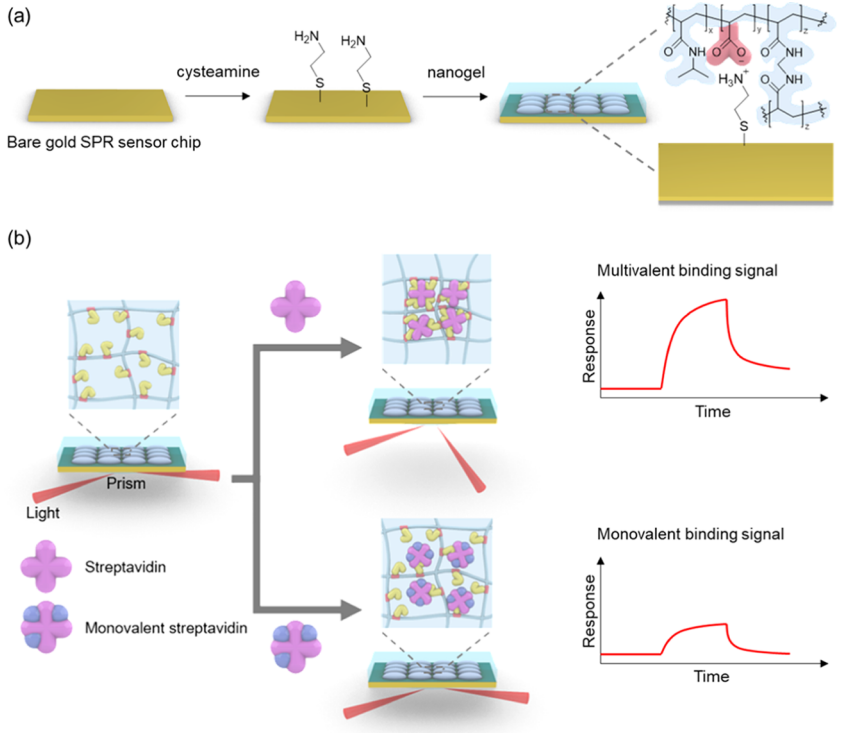

Figure 2. Schematics of the SPR analysis process. (a) Deposition of the nanogels on the surface of a bare gold SPR chip. (b) SPR analysis of monovalent/multivalent analytes with the receptor-functionalized nanogels.

Repligen, Boston, MA) against pure water for 24 h, and the water was changed at the 12 h mark.

2.3. Bioconjugation of the Nanogels. Biosensing capability was imparted to the nanogels by functionalization with receptor molecules (e.g., biocytin, PD-1, or protein A). EDC/NHS coupling was performed to conjugate the amine groups of the receptors to the carboxyl groups of the nanogels. A solution of the nanogels was centrifuged and exchanged for MES buffer (pH 5.6) two times, followed by the addition of EDC (20 mg, 0.65 M) and NHS (40 mg, 1.75 M). The receptor solution (50 μM) was added to the nanogel solution at a concentration of 10% (v/v), and the reaction was kept at room temperature for 40 min. Unreacted EDC/NHS and receptor molecules were removed by centrifuging 5 times, followed by resuspension of the nanogels in the PBS buffer.

2.4. Size and ζ-Potential Measurements. The nanogel particle size and ζ-potential were characterized using a Zetasizer Nano ZS (Malvern Instruments, Worcestershire, UK) equipped with a 633 nm He−Ne laser, and measurements were taken at a 173° detection angle. Disposable polystyrene cuvettes were used for the dynamic light scattering (DLS) measurements, and disposable folded capillary cells were used to perform the ζ-potential measurements. The nanogel sample was allowed to equilibrate at 25 °C for 2 min before size or ζ-potential measurements. The size and ζ-potential data reported were taken from the average of 15 individual measurements with a 10 s integration time for each measurement.

2.5. SPR Analysis. All SPR experiments were conducted with a Biacore T100 apparatus (Biacore GE Healthcare, Chicago, IL) at 25 °C. In the modification of a gold sensor chip, water served as the running buffer for cysteamine functionalization, and 0.1 M MES buffer (0.9% sodium chloride, pH 5.6) served as the running buffer for the nanogel attachment process. In all SPR analyses, PBS served as the running buffer. The sensor chip surface was activated with a 10 mM cysteamine solution in water for 600 s with a flow rate of 2 μL/min. The activated sensor chip was modified with a nanogel solution in the MES buffer 5 times of 60 s injection and 120 s intervals at each cycle (flow rate of 2 μL/min). All the analytes were diluted in the PBS buffer at various concentrations and injected into the chip for 60 s (flow rate of 2 μL/min). The resulting sensorgrams were analyzed by global fitting using an appropriate model in the evaluation program (Biacore Evaluation Program version 2.0).

2.6. Microscopy. Fluorescence microscopy was utilized to observe the Cy2-conjugated streptavidin bound to the biotinylated nanogels. APTMS in ethanol solution (1% v/v) was applied on the plasma-modified glass slide for 1 h, followed by washing with ethanol several times. Next, the biotinylated nanogel solution (20 μL) was dropped on a specific area of the glass slide and incubated for 1 h. The entire glass slide was rinsed with PBS buffer and incubated with 1 μM of Cy2-conjugated streptavidin solution for 10 min. Finally, the glass slide was washed with PBS buffer several times and fluorescence images were captured by an inverted microscope (Nikon, Ti2-E, Tokyo, Japan).

3. RESULTS AND DISCUSSION

First, pNIPAm-*co*-AAc hydrogel nanoparticles were prepared by radical polymerization in water as shown in the scheme (Figure 1a). The molar ratio of *N*-isopropylacrylamide (NIPAm): acrylic acid (AAc): *N*,*N*′-methylenebisacrylamide (BIS) used in the synthesis of the nanogels was 88:10:2. Ammonium persulfate (APS) was used as the initiator, which is decomposed into sulfate anion radicals under heating. Nonionic poly(oxyethylene) sorbitan monooleate (Tween 80) was used as the surfactant and emulsifier. For characterization of the nanogels, NMR spectroscopy was utilized (Figure 1d). Peaks ascribed to the NIPAm and AAc units were observed in the ^{1}H NMR spectrum, and the peaks associated with the cross-linker BIS were not detectable due to its small quantity. The prepared pNIPAm-*co*-AAc nanogels were functionalized by EDC coupling with receptors such as biocytin, Fc-tagged PD-1, and protein A depending on the capturing proteins (herein biocytin) (Figure 1b).

The hydrodynamic sizes of the synthesized pNIPAm-*co*-AAc nanogels and the functionalized nanogels were measured by DLS. There is only one sharp peak in the nanosized area, and it

https://dx.doi.org/10.1021/acsami.9b17328
ACS Appl. Mater. Interfaces 2020, 12, 5413−5419

shows that the neat nanogel is approximately 700 nm in diameter. The polydispersity index (PDI) of the hydrogel is 0.051, which means that the nanogel is very monodispersed in size. The ζ-potential of the neat nanogel shows a negative value because the carboxylate groups in the nanogel networks make the surface charge of the nanogel negative. Additionally, the biotinylated nanogel shows a diameter of approximately 800 nm and a slightly more positive ζ-potential value than that of the neat nanogel (Figure 1c). These phenomena could come from the pH changes and passivation of carboxylate group in the biotinylated nanogels when the neat nanogels underwent EDC coupling step. It has been reported that the size of nanogels in aqueous solution is mostly influenced by charge, cross-linking density, temperature, and pH but not by the addition of mass.[31−33] Moreover, since biocytin is a small molecule, it is unlikely to be explained by the fact that increase in the size of the biotinylated nanogels is solely contributed by the addition of biocytin.

Then, surface functionalization of a bare gold chip was performed to develop a method of using a SPR instrument to measure the MPB in a quantitative and label-free manner (Figure 2a). Cysteamine was utilized to introduce amine functional groups onto the gold chip surface, yielding a positive charge for Coulombic attraction with negatively charged pNIPAm-*co*-AAc nanogels. To maximize the Coulombic force, the plain or functionalized nanogels were dissolved in MES buffer (pH = 5.6), and the resulting solution was injected into an amine-functionalized gold chip in situ. The SPR sensorgrams of each process are shown in the Supporting Information (Figure S1). As a proof of concept to verify the MPB detection capability of our method, we employed a streptavidin−biotin binding system in which a streptavidin molecule is able to bind to four biotin molecules (Figure 2b). Herein, injection of a streptavidin solution into a biotinylated pNIPAm-*co*-AAc nanogel-functionalized gold chip would increase the cross-linking degree of the nanogel network through MPB, which results in deswelling of the nanogels, followed by an increase in the refractive index (RI) of the nanogel layer. The RI change consequently enables the amplification of the intensity of the SPR signal, distinguishing MPB from monovalent binding that has no effect on the cross-linking degree of the nanogel network. In the case of monovalent binding events, a relatively small (or conventional) change in the RI of the nanogel network would be induced by the binding event when monovalent streptavidin was introduced.

A SPR instrument equipped with biotinylated pNIPAm-*co*-AAc nanogel-functionalized gold chips was utilized to measure the response to target proteins including streptavidin, monovalent streptavidin, and bovine serum albumin (BSA) (Figures 3 and S2). It is worth noting that target proteins (e.g., streptavidin) are bound to the biotinylated nanogels in a homogeneous distribution, which was confirmed by using fluorescent Cy2-streptavidin (Figure S3). There is a highly concentration-dependent response of the SPR signals to streptavidin as a model of MPB, while the SPR signals are hardly able to distinguish the concentration difference in monovalent streptavidin at each representative concentration (Figure 3a,b). To compare the SPR response to each sample, we plotted the RUmax (maximum resonance unit) values of streptavidin, monovalent streptavidin, and BSA at each concentration (Figure 3c). As shown in the plot, streptavidin, as a MPB model (black square), shows that the slope of

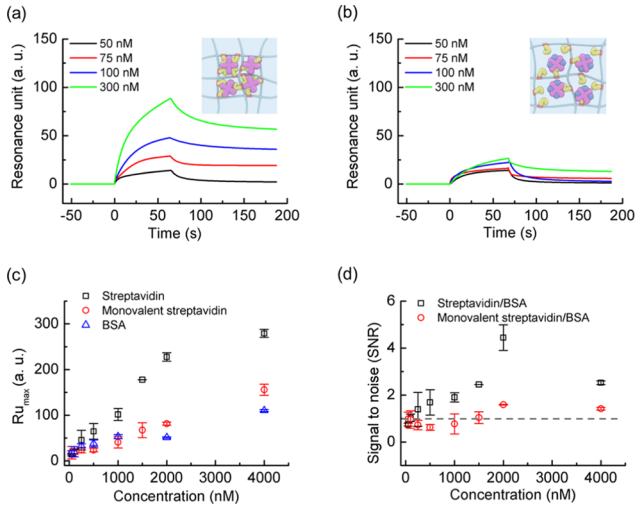

Figure 3. SPR results of the biotinylated nanogels. (a) Sensorgram of streptavidin. (b) Sensorgram of monovalent streptavidin modified with biocytin. (c) Comparison of the maximum SPR signals among streptavidin, monovalent streptavidin, and BSA. (d) Signal-to-noise ratio (SNR) plot from the maximum SPR signals of streptavidin and monovalent streptavidin against those of BSA. Note that the error bars are the standard deviation of three measurements.

RUmax values is ∼3 times higher than that of monovalent streptavidin and BSA. This result indicates that both monovalent streptavidin and BSA, i.e., a nonspecific binding molecule, causes similar SPR responses in their RUmax values, which suggests that our method only enables the production of amplified SPR signals for MPB. To estimate the MPB-enhanced SPR signal, we divided the RUmax values of streptavidin and monovalent streptavidin by those of BSA, a nonspecifically binding protein (Figure 3d). The SNR value of 1 means that there is no difference in the SPR signals of the target molecules from those of nonspecific analytes. The results suggest that our method would be able to detect the target molecule via an MPB event in a complex solution having nonspecific analytes, while the SPR signals of monovalent streptavidin or nonspecific molecules are negligible.

It should be noted that no significant differences in the SPR signal were observed when the detection of multivalent and monovalent streptavidin was conducted using a biotinylated commercial PEG SPR sensor chip (Figure S4). This result shows that the amounts of streptavidin binding to the functionalized surface are similar regardless of its valency. Thus, it suggests that the signal differences between multivalent and monovalent streptavidins in our nanogel system were not due to the difference in the amount of the bound streptavidin.

MPB detection using the SPR signals of bioresponsive nanogel-based gold chips was further examined in an antigen−antibody system (Figures 4 and S5). Each PD-1- and protein A-functionalized nanogel was injected into a gold chip in situ to determine whether the PD-1 IgG antibody binds to the antigens or PD-1 in a multivalent or monovalent manner, respectively. Our experimental approach utilized the fact that each Fab region of a PD-1 IgG antibody can interact with PD-1 proteins with a binding affinity of $K_D = 10^{-9}$,[34] resulting in the formation of the tertiary complex, i.e., MPB. In contrast, the protein A nanogel biochip has a binding affinity ($K_D = 10^{-8}$)[13] only for the Fc region of IgG. With increasing PD-1 IgG concentration, the intensity of the SPR signals changed with

https://dx.doi.org/10.1021/acsami.9b17328
ACS Appl. Mater. Interfaces 2020, 12, 5413−5419

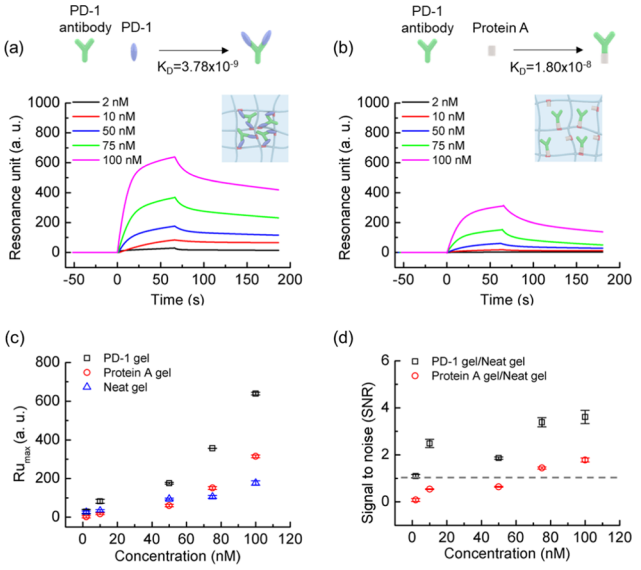

Figure 4. SPR analysis results for PD-1 antibody. (a) Sensorgram of PD-1 functionalized nanogels. (b) Sensorgram of protein A functionalized nanogels. (c) Comparison of the maximum SPR signal among PD-1 nanogels, protein A nanogels, and neat pNIPAm-*co*-AAc nanogels. (d) SNR plot from the maximum SPR signals of PD-1 nanogels and protein A nanogels against the SPR signal of neat pNIPAm-*co*-AAc nanogels. Note that the error bars are the standard deviation of three measurements.

different response degrees, which were higher for the PD-1 nanogel biochips (Figure 4a) than for the protein A biochips (Figure 4b). This result is interesting, considering that the intensity of the SPR signals is subject to changes in the refractive index of the gold chip where the immobilized receptors or ligands are complexed with their binding pairs. Note that we used the same antibody for both measurements. It is also worth mentioning that the kinetic values for both cases were comparable to previously reported values (K_D = 3.78 × 10^{-9} vs K_D = 10^{-9} for PD-1:PD-1 IgG and K_D = 1.80 × 10^{-8} vs K_D = 10^{-8} for Fc of IgG:protein A) (Figure 4a,b). The kinetic values for the binding between PD-1 modified nanogels and PD-1 IgG, calculated from resonance signal using the SPR evaluation system, were demonstrated (Figure S6).

Concurrently, the RUmax and SNR values were also plotted to determine how much the same analyte, PD-1 IgG antibody, induces the different intensities of the SPR signal depending on its binding manner, i.e., multivalent or monovalent. The difference in the RUmax values between the PD-1 nanogel and protein A nanogel systems appeared from a PD-1 IgG concentration of 10 nM, which was two times higher for that of the multivalent system, PD-1 (Figure 4c). In addition, the SNR analysis shows that only the multivalent analyte provides an amplified signal intensity and thereby higher SNR values than those of the monovalent analyte (Figure 4d). Thus, our findings indicate that antigen-modified nanogel biochips are synergistic for the evaluation of antibodies in solution due to amplified SPR signals by MPB formation. Considering SNR values, our method based on MPB would be able to identify a target antibody in solution at a 10-fold lower concentration than that detectable by a conventional method by monovalent binding.

MPB-based analysis using a pNIPAm-*co*-AAc nanogel-modified gold chip and SPR instrument was further expanded for the evaluation of different metal ions (e.g., Na^+, K^+, Ca^{2+}, Fe^{2+}, Fe^{3+}) that have oxidation states of +1, +2, and +3. For 10 μM (Figure 5a) and 1 mM (Figure 5b) solution concentrations, the metal ions in the +2 and +3 oxidation states caused the SPR signals to be amplified to a greater extent than the metal ions in the +1 oxidation state. We postulate that the Ca^{2+}, Fe^{2+}, and Fe^{3+} ions can form MPB-like structures by interacting with carboxylates in the pNIPAm-*co*-AAc nanogel networks, while Na^+ and K^+ are unable to form such MPB-like structures due to the charge valence of the metal ions (Figure 5c). In the SNR plot, it is obvious that metal ions in the +2 and +3 oxidation states display enhanced SNR values in comparison to those of metal ions in the +1 oxidation state (Figure 5d). The difference in binding geometries of metal ions might cause a variation in SPR response, but the effect could be marginal. The size of metal ions (~0.2 nm) is too small compared with that of the nanogels (~700 nm) and carboxylates in the nanogel networks are too flexible to distinguish the binding geometries. Altogether, our results suggest that the use of nanogel-modified SPR analysis allows the evaluation of the oxidation state of metal ions.

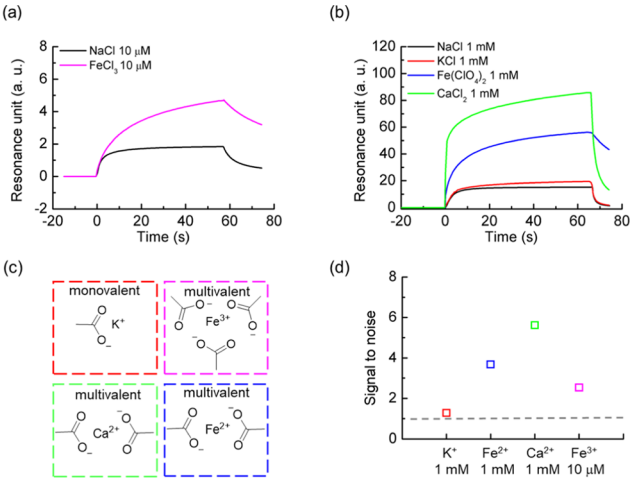

Figure 5. SPR analysis results for metal ions. (a) Response of the neat nanogels to 1 μM metal ions. (b) Response of the neat nanogels to 10 mM metal ions. (c) Interaction concept of metal ions with carboxylate group in the nanogel networks. (d) SNR plot from the RUmax values of metal ions.

4. CONCLUSIONS

In the current study, we demonstrate that the use of bioresponsive pNIPAm-*co*-AAc nanogels to functionalize a SPR gold chip enables the measurement of MPB and its kinetics with no labeling procedure. Our method can produce uniquely amplified SPR signals only at the point where bioresponsive pNIPAm-*co*-AAc nanogels assembled on a SPR gold chip are beginning to form multivalent protein complexes with the target molecules. The magnitude of resonance unit signal tends to increase in proportion to the size of the target molecules (i.e., metal cations < streptavidin < PD-1). Such enhanced signals were not observable from monovalent or nonspecific protein−protein interactions. Using MPB-based SPR analysis, we were able to measure PD-1 IgG antibody at 10 nM with a SNR value above 2, which is at least 3 times higher than that of monovalent SPR analysis by Fc group of PD-1 IgG bound to protein A in our study. There is a caveat that PD-1 IgG antibody has a slightly different K_D for PD-1

https://dx.doi.org/10.1021/acsami.9b17328
ACS Appl. Mater. Interfaces 2020, 12, 5413−5419

and protein A, respectively. The potential merit of our finding is that it hints at the development of a SPR detection system that is capable of analyzing a bispecific or multivalent target molecule from complex media without (or minimized) pretreatment procedures. Furthermore, easy yet accurate detection of MPB and its kinetics opens a new avenue to understand biologically/physiologically important MPB-related systems and thus develop novel types of medical treatment.

■ ASSOCIATED CONTENT

Supporting Information

The Supporting Information is available free of charge at https://pubs.acs.org/doi/10.1021/acsami.9b17328.

SPR data of biochip modification; response of BSA against biotinylated nanogel; and response of PD-1 antibody against the neat nanogel (PDF)

■ AUTHOR INFORMATION

Corresponding Authors

Jongseong Kim − *Korea University, Seoul, Republic of Korea;* orcid.org/0000-0001-9595-2765; Email: envokim72@korea.ac.kr

Dongwon Yoo − *Seoul National University, Seoul, Republic of Korea, and Institute for Basic Science (IBS), Seoul, Republic of Korea;* orcid.org/0000-0002-4547-6948; Email: dwyoo@snu.ac.kr

Other Authors

Hae Min Yang − *Seoul National University, Seoul, Republic of Korea*

Jie Ying Teoh − *Seoul National University, Seoul, Republic of Korea*

Guk Hee Yim − *Seoul National University, Seoul, Republic of Korea*

Yongdoo Park − *Korea University, Seoul, Republic of Korea*

Young Gyu Kim − *Seoul National University, Seoul, Republic of Korea*

Complete contact information is available at: https://pubs.acs.org/10.1021/acsami.9b17328

Author Contributions

The manuscript was written through contributions of all of the authors. All of the authors have given approval to the final version of the manuscript.

Notes

The authors declare no competing financial interest.

■ ACKNOWLEDGMENTS

D.Y. acknowledges financial support by the National Research Foundation of Korea (NRF-2018M3A7B4071204 and NRF-2018R1D1A1A02086125). J.K. acknowledges financial support by the National Research Foundation of Korea (NRF-2016R1D1A1B03933938 and NRF-2019R1I1A1A01057356).

■ REFERENCES

(1) Taylor, I. W.; Wrana, J. L. Protein Interaction Networks in Medicine and Disease. *Proteomics* **2012**, *12*, 1706−1716.

(2) Wu, A. R.; Kawahara, T. L. A.; Rapicavoli, N. A.; Riggelen, Jv.; Shroff, E. H.; Xu, L.; Felsher, D. W.; Chang, H. Y.; Quake, S. R. High Throughput Automated Chromatin Immunoprecipitation as a Platform for Drug Screening and Antibody Validation. *Lab Chip* **2012**, *12*, 2190−2198.

(3) Lyon, L. A.; Musick, M. D.; Natan, M. J. Colloidal Au-Enhanced Surface Plasmon Resonance Immunosensing. *Anal. Chem.* **1998**, *70*, 5177−5183.

(4) Hitomi, Y.; Outten, C. E.; O'Halloran, T. V. Extreme Zinc-Binding Thermodynamics of the Metal Sensor/Regulator Protein, ZntR. *J. Am. Chem. Soc.* **2001**, *123*, 8614−8615.

(5) Toma, M.; Jonas, U.; Mateescu, A.; Knoll, W.; Dostalek, J. Active Control of SPR by Thermoresponsive Hydrogels for Biosensor Applications. *J. Phys. Chem. C* **2013**, *117*, 11705−11712.

(6) Tsai, C.-t.; Robinson, P. V.; Cortez, F. dJ.; Elma, M. L. B.; Seftel, D.; Pourmandi, N.; Pandori, M. W.; Bertozzi, C. R. Antibody Detection by Agglutination−PCR (ADAP) Enables Early Diagnosis of HIV Infection by Oral Fluid Analysis. *Proc. Natl. Acad. Sci. U.S.A.* **2018**, *115*, 1250−1255.

(7) Salazar-Alvarez, M.; Korostynska, O.; Mason, A.; Al-Shamma'a, A.; Cooney, J. C.; Magner, E.; Tofail, S. A. Label Free Detection of Specific Protein Binding Using a Microwave Sensor. *Analyst* **2014**, *139*, 5335−5338.

(8) Li, H.; Rothberg, L. J. Label-Free Colorimetric Detection of Specific Sequences in Genomic DNA Amplified by the Polymerase Chain Reaction. *J. Am. Chem. Soc.* **2004**, *126*, 10958−10961.

(9) Fan, X.; White, I. M.; Shopova, S. I.; Zhu, H.; Suter, J. D.; Sun, Y. Sensitive Optical Biosensors for Unlabeled Targets: a Review. *Anal. Chim. Acta* **2008**, *620*, 8−26.

(10) Kuznetsova, V. E.; Spitsyn, M. A.; Shershov, V. E.; Guseinov, T. O.; Fesenko, E. E.; Lapa, S. A.; Ikonnikova, A. Y.; Avdonina, M. A.; Nasedkina, T. V.; Zasedatelev, A. S.; Chudinov, A. V. Novel Fluorescently Labeled Nucleotides: Synthesis, Spectral Properties and Application in Polymerase Chain Reaction. *Mendeleev Commun.* **2016**, *26*, 95−98.

(11) Berggård, T.; Linse, S.; James, P. Methods for the Detection and Analysis of Protein−Protein Interactions. *Proteomics* **2007**, *7*, 2833−2842.

(12) Braun, P.; Gingras, A.-C. History of Protein-Protein Interactions: From Egg-White to Complex Networks. *Proteomics* **2012**, *12*, 1478−1498.

(13) Choe, W.; Durgannavar, T.; Chung, S. Fc-Binding Ligands of Immunoglobulin G: An Overview of High Affinity Proteins and Peptides. *Materials* **2016**, *9*, No. 994.

(14) Farr, G. W.; Furtak, K.; Rowland, M. B.; Ranson, N. A.; Saibil, H. R.; Kirchhausen, T.; Horwich, A. L. Multivalent Binding of Nonnative Substrate Proteins by the Chaperonin GroEL. *Cell* **2000**, *100*, 561−573.

(15) Ghiotto, M.; Gauthier, L.; Serriari, N.; Pastor, S.; Truneh, A.; Nunes, J. A.; Olive, D. PD-L1 and PD-L2 Differ in Their Molecular Mechanisms of Interaction with PD-1. *Int. Immunol.* **2010**, *22*, 651−660.

(16) Dahle, C.; Skogh, T.; Åberg, A. K.; Jalal, A.; Olcén, P. Methods of Choice for Diagnostic Antinuclear Antibody (ANA) Screening. *J. Autoimmun.* **2004**, *22*, 241−248.

(17) Zhang, S.; Zhang, M.; Wu, W.; Yuan, Z.; Tsun, A.; Wu, M.; Chen, B.; Li, J.; Miao, X.; Miao, X.; Liu, X.; Yu, D.; Liu, J. Preclinical Characterization of Sintilimab, a Fully Human anti-PD-1 Therapeutic Monoclonal Antibody for Cancer. *Antibody Ther.* **2018**, *1*, 45−53.

(18) Sasaki, T.; Hiroki, K.; Yamashita, Y. The Role of Epidermal Growth Factor Receptor in Cancer Metastasis and Microenvironment. *Biomed. Res. Int.* **2013**, *2013*, No. 546318.

(19) Pierce, M. M.; Raman, C. S.; Nall, B. T. Isothermal Titration Calorimetry of Protein-Protein Interactions. *Methods* **1999**, *19*, 213−221.

(20) Velazquez-Campoy, A.; Leavitt, S. A.; Freire, E. Characterization of Protein-Protein Interactions by Isothermal Titration Calorimetry. *Methods Mol. Biol.* **2004**, *261*, 35−54.

(21) Drescher, D. G.; Ramakrishnan, N. A.; Drescher, M. J. Surface Plasmon Resonance (SPR) Analysis of Binding Interactions of Proteins in Inner-ear Sensory Epithelia. *Methods Mol. Biol.* **2009**, *493*, 323−343.

(22) Canovi, M.; Lucchetti, J.; Stravalaci, M.; Re, F.; Moscatelli, D.; Bigini, P.; Salmona, M.; Gobbi, M. Applications of Surface Plasmon Resonance (SPR) for the Characterization of Nanoparticles Developed for Biomedical Purposes. *Sensors* **2012**, *12*, 16420−16432.
(23) Hearty, S.; Leonard, P.; O'Kennedy, R. Measuring Antibody-Antigen Binding Kinetics Using Surface Plasmon Resonance. *Methods Mol. Biol.* **2012**, *907*, 411−442.
(24) Lynch, H. E.; Stewart, S. M.; Kepler, T. B.; Sempowski, G. D.; Alam, S. M. Surface Plasmon Resonance Measurements of Plasma Antibody Avidity during Primary and Secondary Responses to Anthrax Protective Antigen. *J. Immunol. Methods* **2014**, *404*, 1−12.
(25) Mateescu, A.; Wang, Y.; Dostalek, J.; Jonas, U. Thin Hydrogel Films for Optical Biosensor Applications. *Membranes* **2012**, *2*, 40−69.
(26) Hoare, T. R.; Kohane, D. S. Hydrogels in Drug Delivery: Progress and Challenges. *Polymer* **2008**, *49*, 1993−2007.
(27) Li, J.; Mooney, D. J. Designing Hydrogels for Controlled Drug Delivery. *Nat. Rev. Mater* **2016**, *1*, 16071.
(28) Zhou, Y.; Wan, C.; Yang, Y.; Yang, H.; Wang, S.; Dai, Z.; Ji, K.; Jiang, H.; Chen, X.; Long, Y. Highly Stretchable, Elastic, and Ionic Conductive Hydrogel for Artificial Soft Electronics. *Adv. Funct. Mater.* **2019**, *29*, No. 1806220.
(29) Kim, J.; Park, Y.; Brown, A. C.; Lyon, L. A. Direct Observation of Ligand-Induced Receptor Dimerization with a Bioresponsive Hydrogel. *RSC Adv.* **2014**, *4*, 65173−65175.
(30) Tyburski, E. A.; Gillespie, S. E.; Stoy, W. A.; Mannino, R. G.; Weiss, A. J.; Siu, A. F.; Bulloch, R. H.; Thota, K.; Cardenas, A.; Session, W.; Khoury, H. J.; O'Connor, S.; Bunting, S. T.; Boudreaux, J.; Forest, C. R.; Gaddh, M.; Leong, T.; Lyon, L. A.; Lam, W. A. Disposable Platform Provides Visual and Color-based Point-of-Care Anemia Self-testing. *J. Clin. Invest.* **2014**, *124*, 4387−4394.
(31) Kim, J.; Nayak, S.; Lyon, L. A. Bioresponsive Hydrogel Microlenses. *J. Am. Chem. Soc.* **2005**, *127*, 9588−9592.
(32) Lee, S. K.; Hwang, G.; Woo, J.; Park, J.; Kim, J. Characterization of Responsive Hydrogel Nanoparticles upon Polyelectrolyte Complexation. *Polymers* **2017**, *9*, No. 66.
(33) Lee, S.-K.; Park, Y.; Kim, J. Thermoresponsive Behavior of Magnetic Nanoparticle Complexed pNIPAm-co-AAc Microgels. *Appl. Sci.* **2018**, *8*, No. 1984.
(34) Tan, S.; Zhang, H.; Chai, Y.; Song, H.; Tong, Z.; Wang, Q.; Qi, J.; Wong, G.; Zhu, X.; Liu, W. J.; Gao, S.; Wang, Z.; Shi, Y.; Yang, F.; Gao, G. F.; Yan, J. An Unexpected N-terminal Loop in PD-1 Dominates Binding by Nivolumab. *Nat. Commun.* **2017**, *8*, No. 14369.

https://dx.doi.org/10.1021/acsami.9b17328
ACS Appl. Mater. Interfaces 2020, 12, 5413−5419